ResearchGate

See discussions, stats, and author profiles for this publication at: https://www.researchgate.net/publication/41410794

Theoretical Study on the Reaction Mechanism between 6-Benzyl-6-azabicyclo[2.2.1]hept-2-ene and Benzoyl Isocyanate to Urea and Isourea

ARTICLE *in* THE JOURNAL OF PHYSICAL CHEMISTRY A · FEBRUARY 2010

Impact Factor: 2.69 · DOI: 10.1021/jp910173d · Source: PubMed

CITATIONS
15

READS
13

6 AUTHORS, INCLUDING:

Yanyan Zhu
Zhengzhou University
55 PUBLICATIONS **611** CITATIONS
SEE PROFILE

Donghui Wei
Zhengzhou University
65 PUBLICATIONS **512** CITATIONS
SEE PROFILE

Mingsheng Tang
Zhengzhou University
95 PUBLICATIONS **1,380** CITATIONS
SEE PROFILE

Available from: Donghui Wei
Retrieved on: 24 January 2016

Theoretical Study on the Reaction Mechanism between 6-Benzyl-6-azabicyclo[2.2.1]hept-2-ene and Benzoyl Isocyanate to Urea and Isourea

Cong Zhang, Yanyan Zhu,* Donghui Wei, Dongzhen Sun, Wenjing Zhang, and Mingsheng Tang*

Center of Computational Chemistry, Department of Chemistry, Zhengzhou University, Zhengzhou, Henan Province, 450052, P. R. China

Received: October 24, 2009; Revised Manuscript Received: January 20, 2010

Reaction mechanisms of the 6-benzyl-6-azabicyclo[2.2.1]hept-2-ene with benzoyl isocyanate have been investigated using density functional theory (DFT) at the B3LYP/6-31G(d,p) level of theory. The reaction proceeding along six competitive channels includes two categories. That is, two channels are formally [3,3]-sigmatropic rearrangements and four channels are [4+2] cycloadditions. For urea, the formally [3,3]-sigmatropic rearrangement channel and the [4+2] cycloaddition channels are competitive since they have similar barriers. However, the [4+2] cycloaddition channels are energetically favorable pathways to lead to isourea, with the highest barrier of 12.77 kcal/mol. These polar Diels−Alder (P-DA) reactions are controlled by the charge transfer (CT) at the transition states. Moreover, the main products of this reaction include urea and isourea. Furthermore, difference of two new bond lengths at transition states indicate that the [4+2] cycloadditions in this reaction are asynchronous processes, which is in good agreement with the experiment.

Introduction

Urea and its analogs have attracted considerable interest in relation to their diverse potentials not only as antitumor agents but also in economic developments in recent years.[1−3] Since urea was first synthesized in 1828,[4−6] the urea family has been extensively studied by using both experiments and theoretical calculations due to their special structures and reaction activities.[7−14] For example, Bukuo Ni has designed and synthesized nine chiral room-temperature pyridinium ionic liquids, which contain a urea to a chiral moiety tethered unit.[15] Tris-urea with low molecular weight gelators was synthesized in three steps from 1,3,5-tris(bromomethyl)-2,4,6-triethylbenzene in 82% to 88% yields by Yamanaka.[16]

Particularly, urea and isourea can act as the chiral catalysts for asymmetric reaction,[17−20] since they have three coordination sites (one oxygen and two nitrogen atoms) and they are able to form complexes of different coordination numbers with several metals.[21−23] For instance, Lee reported the chiral bifunctional urea catalyzed the reactions of α-cyano ketones with *N*-Boc aldimines.[24] Moreover, aqueous urea solutions are widely used for protein denaturation.[25,26] Loggio has researched the urea-induced denaturation process on defatted human serum albumin and in the presence of palmitic acid.[27] Additionally, urea is very important for agricultural practicality because it is an easy source of nitrogenous fertilizer to the vegetable kingdom through a simple enzymatic hydrolysis with the aid of urease.[28]

Noteworthy, more recently, Madalengoitia and his co-workers[29,30] have reported that the 6-benzyl-6-azabicyclo[2.2.1] hept-2-ene with benzoyl isocyanate afforded urea (assigned as **P1** in Scheme 1) and isourea (assigned as **P2** in Scheme 1) without catalyst at room temperature.[31] However, as shown in Scheme 1, how the reaction can happen, and why the main products involve **P1** and **P2**, in which the yield of **P1** is more than that of **P2**, are a difficult subject to understand essentially these important information mentioned above, unless we can obtain more details at the molecular level.

SCHEME 1

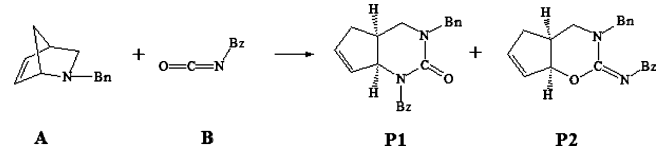

In this work, the compounds **A** (6-benzyl-6-azabicyclo[2.2.1]-hept-2-ene) and **B** (benzoyl isocyanate), as shown in Scheme 1, were chosen as the objects of investigation, and the reaction mechanisms in the different reaction channels were studied using density functional theory, which has been widely used in the study of the mechanism.[32−35]

Computational Details

All geometries for the studied complexes were fully optimized at the B3LYP/6-31G(d,p) level[36−38] of theory. Compared with other levels of theory, the B3LYP method was sufficiently accurate for predicting reliable geometries and frequencies of the stationary points.[39−42] The optimized reactants, intermediates and product structures reported in this paper show positive eigenvalues of the Hessian matrix, whereas transition states (TSs) have one and only one negative eigenvalue. To corroborate which are the correspondent minima linked by the considered TS, normal coordinate analysis is performed on these TS structures by intrinsic reaction coordinate (IRC) routes[43] in both reactant and product directions. The electronic properties of the complexes were discussed using the natural bond orbital (NBO) analysis at the same level by the NBO 3.1 program.[44] The solvent effect (chloroform chosen from the available experiment[31]) is also considered. The polarizable continuum model (PCM)[45−49] has been used to simulate the solvent effect as implemented within the solvent reaction field using the

* Corresponding authors. Y.Y.Z.: e-mail, zhuyan@zzu.edu.cn. M.S.T., e-mail: mstang@zzu.edu.cn.

10.1021/jp910173d © 2010 American Chemical Society
Published on Web 02/08/2010

SCHEME 2: Proposed Mechanisms for the Title Reaction

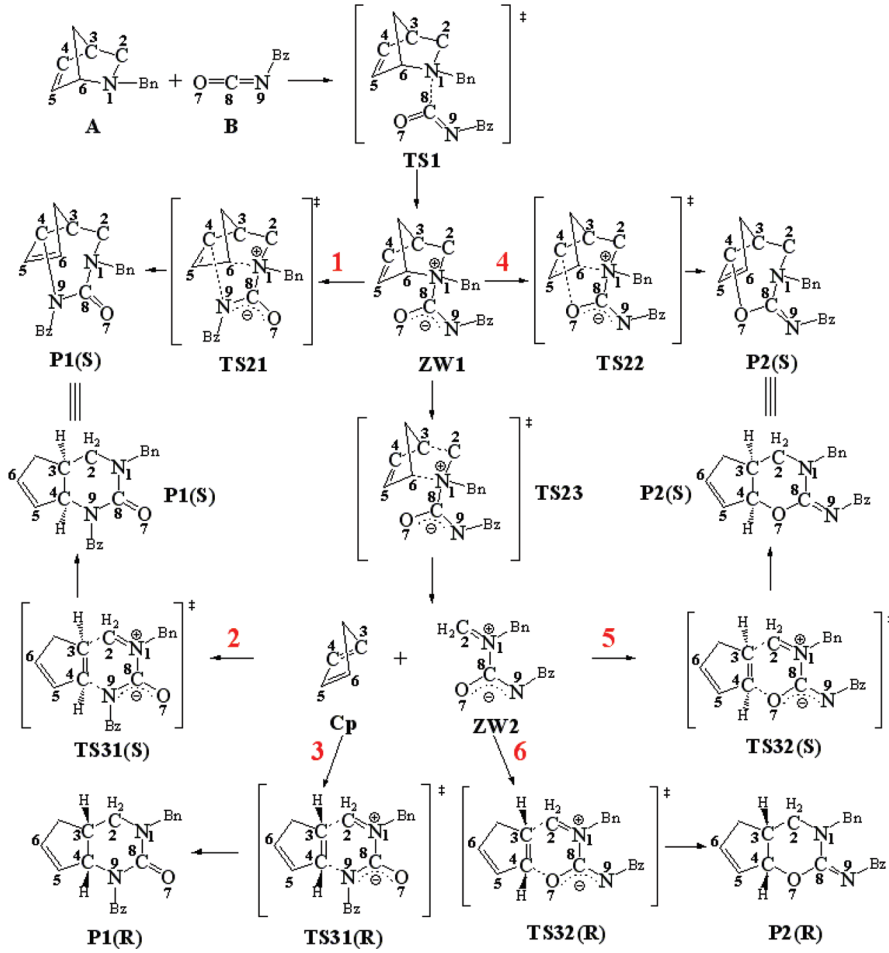

optimized structures in chloroform solvent. All theoretical calculations were performed using the Gaussian03 program package.[50]

Results and Discussion

Based on experimental results,[31] several possible channels for the title reaction were proposed, including [3,3]-sigmatropic rearrangement and [4+2] cycloaddition, as presented in Scheme 2, to investigate the reaction mechanism. It can be seen from Scheme 2, reactant **A** reacts with **B** to generate an important intermediate **ZW1** that can be converted into different products through two different ways: [3,3]-sigmatropic rearrangement (channels 1 and 4) and [4+2] cycloaddition (channels 2, 3, 5, and 6).

1. Generation of ZW1. The reaction is initiated by the nucleophilic attack of the tertiary amine **A** to the electrophilically activated carbon of benzoyl isocyanate **B** with formation of **ZW1**. The optimized structures of **A**, **B**, and **ZW1** are shown in Figure 1. It can be observed that the N1−C8 bond length was shortened from 2.039 Å in **TS1** to 1.711 Å in **ZW1**, indicating that the reactant **A** becomes closer to **B**. The large distance of the N1−C8 bond length at **ZW1** presents a coordinate bond. The energy profile of the channel to **ZW1** is shown in Figure 2. The energy of **TS1** lies 6.67 kcal/mol above that of the reactants (**A** and **B**), which is a low-energy barrier at room temperature. Furthermore, the NBO charge analysis indicates that there is 0.45 e charge transfer from **A** to **B** in **ZW1**.

Subsequently, from **ZW1** to **P1/P2**, six channels were suggested to investigate the reaction process. Each channel could be illustrated as follows:

2. Ways to P1(S&R). There could be three channels to **P1(S&R)**. **P1(S)** could be obtained via channels 1 and 2, and **P1(R)** could be obtained via channel 3 (as shown in Scheme 2).

Channel 1: [3,3]-Sigmatropic Rearrangement Mechanism. There is only one step in channel 1; actually, channel 1 is a formally [3,3]-sigmatropic rearrangement, which is the rearrangement of zwitterionic species **ZW1** to a more stable neutral one **P1(S)**. That is, the N9 atom attacks on the C4 atom while the N1−C6 bond breaks. From Figure 1, at **TS21**, the distance of N1−C6 is elongated to 2.281 Å. Simultaneously, the distance of C4−N9 is shortened from 2.814 Å in **TS21** to 1.493 Å in **P1(S)**. Notably, since the N9 atom is under the planar alkene, which causes the N9 atom to approach the C4 atom from only one orientation, it seems possible to obtain the only product **P1(S)**. Moreover, the energies of stationary points in channel 1 are shown in Figure 2. Obviously, the barrier of the rate-determined step of channel 1 is 12.03 kcal/mol, which is in good agreement with the experimental condition that the reaction could proceed at room temperature. The energy of **P1(S)** is 40.32 kcal/mol lower than those of the reactants, demonstrating that this process is strongly exothermic. Furthermore, the changes of the main geometric parameters and energies along the channel 1 are depicted in Figure 3. It reveals that the key evolvement of the geometric parameters is on the distance of N1−C6, which contributes to the energy barrier for the reaction. From the above

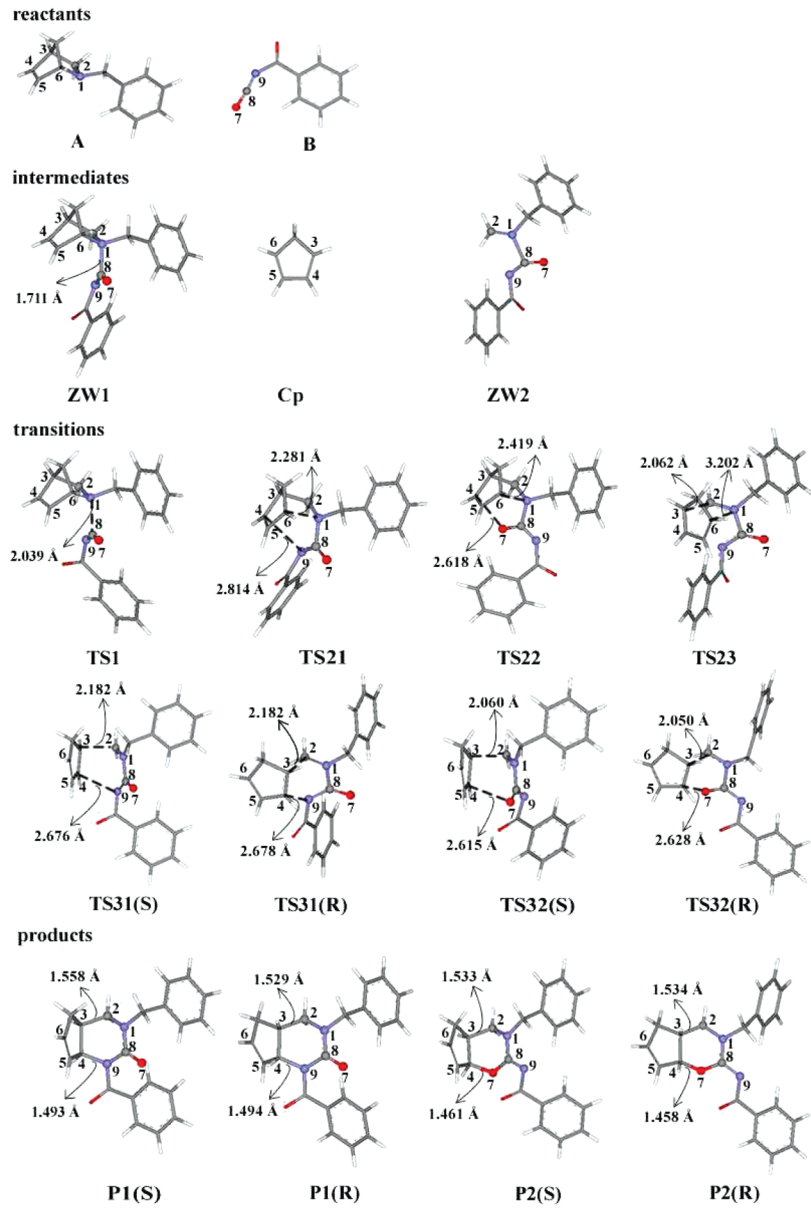

Figure 1. Optimized structures of reactants, intermediates, transition states, and products in the reaction.

analysis, it is revealed that the N1−C6 breaking bond and the C4−N9 forming bond indicate that the rearrangement is promoted by the cationic N1 atom of **ZW1**.

Channel 2: [4+2] Cycloaddition Mechanism. There are two steps in the reaction channel 2 (see Scheme 2): This channel is initialized by a retro-Diels−Alder (retro-DA) reaction at **ZW1** to yield cyclopentadiene (**Cp**) and a new zwitterionic intermediate (**ZW2**). Then, the next step is [4+2] cycloaddition between **Cp** and **ZW2** whose product is **P1(S)**. The optimized structures of **TS23**, **Cp**, **ZW2**, and **TS31(S)** in channel 2 are shown in Figure 1. At **TS23**, the N1−C6 and C2−C3 bonds are nearly broken, and their bond lengths are elongated to 2.062 and 3.202 Å, respectively. At **ZW2**, the dihedral angels of C2−N1−C8−N9 and C2−N10−C8−O7 are +11.04° and −171.14°, respectively, implying that these five atoms are almost in the same plane. At **TS31(S)**, both the C3 atom and the C4 atom are in the **S** configuration, in which the distances of C2−C3 and C4−N9 are 2.182 and 2.676 Å, respectively. The extent of the asynchronicity of the bond formation can be gauged by the difference between the lengths of the bonds being formed in the reaction[51−55] $\Delta r = d(\text{C4}-\text{N9}) - d(\text{C3}-\text{C2})$. According to previous report, the obtained value of Δr is 0.494 Å in this work, indicating that the cycloaddition is an asynchronous process. At last, the two bonds of C3−C2 and C4−N9 have fully formed in **P1(S)** with lengths of 1.529 and 1.493 Å, respectively.

The global electrophilicity character of a molecule is measured by the electrophilicity index,[56−61] ω, which has been given from the following equation, $\omega = \mu^2/2\eta$, in terms of the electronic chemical potential μ and the chemical hardness η. Both quantities may be approached in terms of the one-electron energies of the frontier molecular orbital HOMO and LUMO, ε_H and ε_L, as $\mu \approx (\varepsilon_H + \varepsilon_L)/2$ and $\eta \approx \varepsilon_L - \varepsilon_H$.[58−61] Moreover, Domingo and co-workers have introduced a nucleophilicity index,[62] N, on the basis of the HOMO energies obtained within the Kohn−Sham scheme,[63] and defined as $N = E_{\text{HOMO(Nu)}} - E_{\text{HOMO(TCE)}}$.[62] This nucleophilicity scale is referred to tetracyanoethylene (TCE) taken as a reference. Followed these indices definition, **Cp** is a marginal electrophile ($\omega = 0.83$ eV) classified as a good nucleophile[60,62,64] ($N = 3.35$ eV). The large electrophilic character of the zwitterionic intermediate **ZW2**, $\omega = 2.15$ eV, means that it could participate as a good electrophile in a polar Diels−Alder (P-DA) reaction.[65] Along the nucleophilic

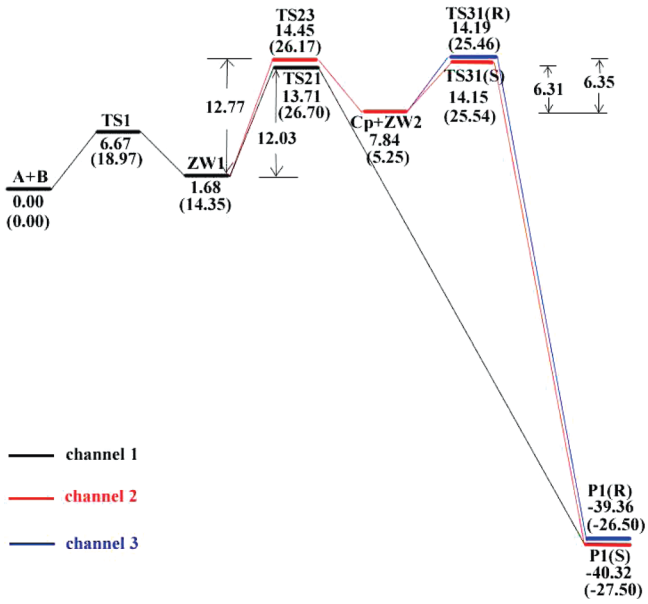

Figure 2. Energy (kcal/mol) profiles of channels 1, 2, and 3 along with the free energies (in parentheses).

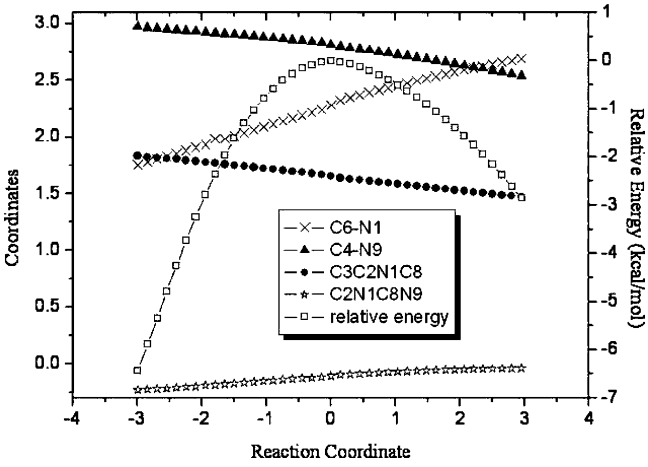

Figure 3. Relative energy (kcal/mol) for the conversion of **ZW1** to **P1(S)** and main geometric parameters of stationary points along the reaction pathway (here bond length in Å and dihedral angle in radian).

attack of **Cp** to the C2 atom of **ZW2** begins a retrodonation from the negatively charged N9 atom of **ZW2** to the C4 position of the incipient C3−C4−C6 allyl cation, which develops along the nucleophilic attack of **Cp** to **ZW2**. This behavior is in agreement with the large nucleophilic character of **Cp**. Furthermore, according to the NBO analysis, the charge transfer (CT) found at **TS31(S)**, 0.24 e, is in agreement with the polar nature (0.20 e < CT < 0.40 e)[65] of these cycloadditions. The low CT and asynchronicity found at these P-DA reactions relative to the ionic Diels−Alder reaction[65,66] is a consequence of the zwitterionic character of **ZW2**.

In channel 2, the energy barrier of the bond breaking in first step is 12.77 kcal/mol (see Figure 2) and the energy barrier of the [4+2] cycloaddition process is only 6.31 kcal/mol. Therefore, the rate-determined step in this pathway occurs in the first step that **ZW1** is decomposed to **Cp** and **ZW2**. Additionally, these energy barriers are resonable since this channel is a P-DA reaction.

Channel 3: [4+2] Cycloaddition Mechanism. Due to the free N1−C8 bond rotation at **ZW2**, there is an exo addition between **Cp** and **ZW2** in channel 3. The stationary points, **TS31** and **P1(R)**, in channel 3 are shown in Figure 1. At **TS31(R)**, both the C3 atom and the C4 atom are in the **R** configuration. The distances of C3−C2 and C4−N9 are 2.182 and 2.678 Å in **TS31(R)**, respectively. The value of Δr is 0.496 Å, which indicates that the cycloaddition is also an asynchronous process. At **P1(R)**, the C2−C3 and C4−N9 bonds are shortened to 1.529 and 1.494 Å, respectively, demonstrating that the two bonds have fully formed. In addition, the large charge transfer (CT) found at **TS31(R)** in the P-DA process, 0.23 e, is consistent with the polar nature of the cycloaddition.[65]

In channel 3, the energy barrier of the first step is the same as that of channel 2, which is 12.77 kcal/mol (see Figure 2). For a similar [4+2] cycloaddition, the energy barrier of the second step is 6.35 kcal/mol, which is very close to that of channel 2. Additionally, these energy barriers are resonable since this channel is a P-DA reaction. Furthermore, the energy of **P1(R)** is −39.36 kcal/mol, being 0.96 kcal/mol above that of **P1(S)** and the process is exothermic.

Taking the three channels (channels 1, 2, and 3) into account, the energy barrier of the rate-determined step for channel 1, 12.03 kcal/mol, is very similar to the highest energy barrier of channels 2 and 3 (12.77 kcal/mol). It is interesting to note that the free energies of these three channels are very close. On the basis of the information mentioned above, it is deduced that channels 1, 2, and 3 are competitive pathways. That is to say, the product **P1** could be obtained through [3,3]-sigmatropic rearrangement (channel 1) and [4+2] cycloaddition (channels 2 and 3).

3. Ways to P2(S&R). Similar to **P1(S&R)**, **P2(S&R)** are also obtained through three suggested pathways: one [3,3]-sigmatropic rearrangement (denoted as channel 4) and two [4+2] cycloaddition mechanisms (denoted as channels 5 and 6) (as shown in Scheme 2).

Channel 4: [3,3]-Sigmatropic Rearrangement Mechanisms. Similarly, channel 4 is not a pericyclic process but a rearrangement of **ZW1** to a more stable neutral one **P2(S)**. But in channel 4, the process is the O7 atom attacking on the C4 atom with the bond of N1−C6 breaking,[67,68] which clearly shows the bond of C4−O7 formation in **P2(S)** via **TS22** (as shown in Scheme 2). At **TS22**, the distance of N1−C6 is elongated to 2.419 Å. The bond length of C4−O7 is shortened from 2.618 Å in **TS22** to 1.461 Å in **P2(S)** (as shown in Figure 1). Similar to channel 1, the N1−C6 breaking bond and the C4−O7 forming bond also indicate that the rearrangement is promoted by the cationic N1 atom of **ZW1**. Just as channel 1, the O7 atom lies under the planar alkene, resulting that the O7 atom could approach the C4 atom from only one orientation to obtain the only product **P2(S)**.

Figure 4 shows the energies of stationary points involved in channel 4. It can be seen that the energy barrier of the rate-determined step in channel 4 is 18.87 kcal/mol, which is 6.84 kcal/mol higher than that of channel 1. And the product **P2(S)** is 24.11 kcal/mol lower than those of the reactants in this channel, which indicates that the process is exothermic. This energy difference relative to that for channel 1 could be rationalized by the larger nucleophilic character of the N9 nitrogen atom than the O7 oxygen atom at the zwitterionic intermediate **ZW1**.

Channel 5: [4+2] Cycloaddition Mechanisms. Two steps in channel 5 are similar to those of channel 2 (see Scheme 2). The first step is also the R-DA process, in which **ZW1** divides into **Cp** and **ZW2**. The second step is the cycloaddition, which is accomplished by the bonds of C4−O7 and C2−C3 formation via **TS32(S)**. At **TS32(S)**, both the C3 atom and the C4 atom

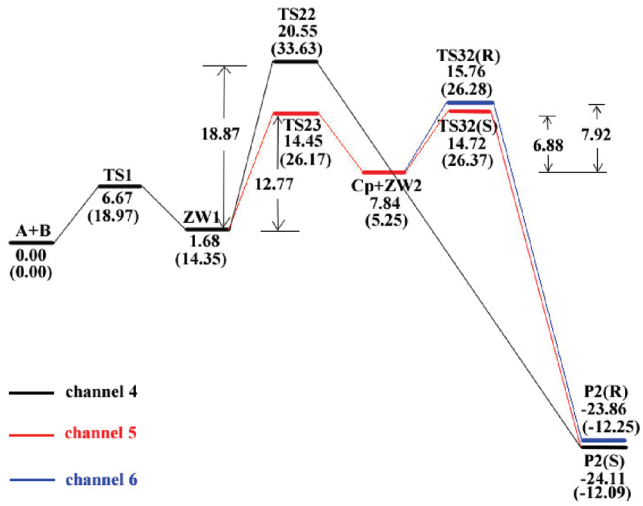

Figure 4. Energy (kcal/mol) profiles of channels 4, 5, and 6 along with the free energies (in parentheses).

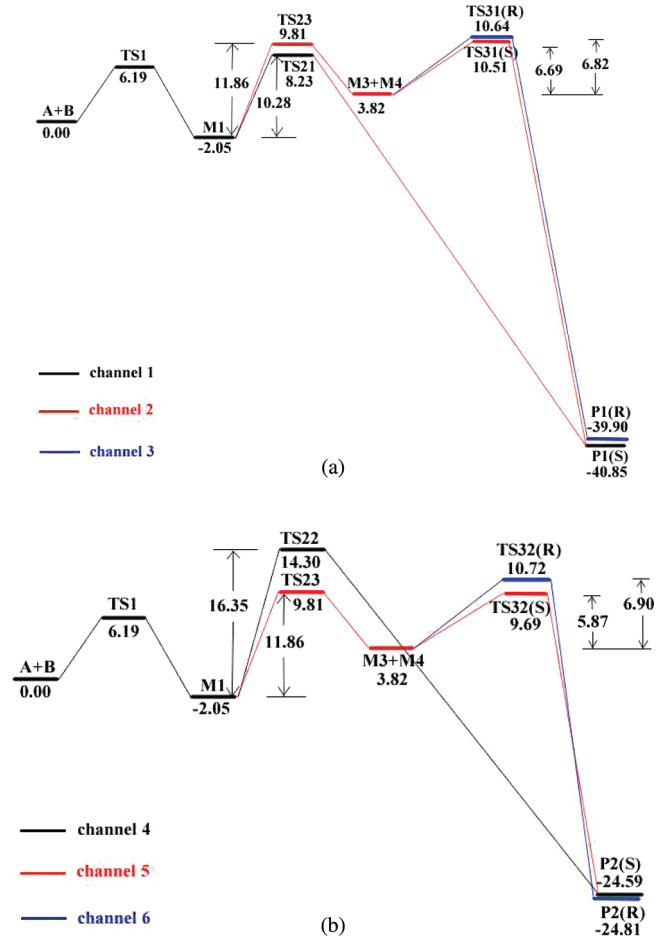

Figure 5. Energy (kcal/mol) profiles of six channels in chloroform: (a) for channels 1, 2, and 3; (b) for channels 4, 5, and 6.

are in the **S** configuration. Moreover, at **TS32(S)**, the distances of C3−C2 and C4−O7 are 2.060 and 2.615 Å (as shown in Figure 1), respectively. In this channel, $\Delta r = d(\text{C4−O7}) - d(\text{C3−C2}) = 0.555$ Å, indicating that the cycloaddition is an asynchronous process, in which the bond of C2−C3 forms faster than the bond of C4−O7. The bonds of C3−C2 and C4−O7 are finally formed in **P2(S)**. Similar to channel 2, the value of the charge transfer at **TS32(S)** is 0.33 e, which is in agreement with the nature of the P-DA cycloaddition.[65]

The energy barrier of the first step is also 12.77 kcal/mol in channel 5, as shown in Figure 4. And the energy barrier of the cycloaddition process is only 6.88 kcal/mol. The energy barrier of the rate-determined step of channel 5 is 6.10 kcal/mol lower than that of channel 4.

Channel 6: [4+2] Cycloaddition Mechanisms. The first step of channel 6 is that **ZW1** is decomposed into **Cp** and **ZW2**, which is the same as channel 5, as shown in Scheme 2. However, the last step is also a cycloddition process between **Cp** and **ZW2**, which is an exo addition process. At **TS32(R)**, both the C3 atom and the C4 atom are in the **R** configuration. The distances of C3−C2 and C4−O7 are 2.050 and 2.628 Å, respectively, and the value of Δr is 0.578 Å, indicating that the second step is an asynchronous process. The bonds of C3−C2 and C4−O7 have fully formed in **P2(R)** with the bond lengths 1.534 and 1.458 Å, respectively (as shown in Figure 1). In the cycloddition process, 0.36 e is transferred at **TS32(R)**, which is consistent with the P-DA character.[65] Furthermore, the energy barrier of the first step in channel 6 is 12.77 kcal/mol, which is the same as that of channel 5 (as presented in Figure 4). And the second energy barrier is 7.92 kcal/mol in channel 6, which is slightly higher (1.04 kcal/mol) than that of channel 5.

Taking the three channels (channels 4, 5, and 6) into consideration, the same energy barrier of the rate-determined step in channels 5 and 6 is 6.10 kcal/mol lower than that of channel 4. The free energy of **TS23** involved in channels 5 and 6 is 7.76 kcal/mol lower than that of **TS22** involved in channel 4 (see Figure 4). Note also that the second energy barrier and free activation energy barrier in channel 5 are close to those of channel 6. The calculated results deduced that **P2** could be obtained through the [4+2] cycloaddition mechanism.

Taking all channels into account, this reaction is a domino process that compresses several polar reactions. The reaction is initiated by the nucleophilic attack of **A** to the electrophilically activated carbon of **B** with formation of **ZW1**. This intermediate is not stable and it can trace two competitive channels. Through the reaction channels 1 and 4, **ZW1** is converted in **P1** and **P2**. These rearrangements take place via high asynchronous TSs, in which the N1−C6 breaking bond is more advanced than the C4−N9(O7) forming bond. The positively charged N1 nitrogen atom of **ZW1**, which assists the heterolitic N1−C6 cleavage, promotes these rearrangements. The concomitant nucleophilic attack of the negatively charged O7 or N9 of the benzoyl isocyanate residue to the C4 position of the C4−C5−C6 allyl cation framework allows the formation of **P1** and **P2**. Through the reaction channels 2 and 3 and 5 and 6, **ZW1** is converted in the **R** and **S** configurations of **P1** and **P2**, respectively, via a retro-DA// P-DA domino reaction. For **P1**, the energy barriers and free energy barriers of the [3,3]-sigmatropic rearrangement mechanism and the [4+2] cycloaddition mechansims are so close that these two mechanisms could occur to yield **P1**. But for **P2**, the energy barriers of the two [4+2] cycloadditions are obviously lower than that of the [3,3]-sigmatropic rearrangement, which is in agreement with the free energy profile. Moreover, the energy of**P1** is lower than that of **P2**. All these calculations are good consistent with the experimental results.

4. Solvent Effect. To consider the role of the solvent, energies of stationary points in chloroform are carried out using the PCM model as presented in Figure 5. As shown in Figure 5a, in the chloroform solvent, the energies of all stationary points are decreased in a small extent. The energy barrier of the rate-determined step in channel 1 (10.28 kcal/mol) is lower than those of channels 2 and 3 (11.86 kcal/mol), which indicates

that channel 1 is an energy favorable channel. From Figure 5b, for the **P2(S&R)** generation, the energy barrier of the rate-determined step in channel 4 is 16.35 kcal/mol. For channels 5 and 6, the energy barrier of the rate-determined step is 11.86 kcal/mol. However, the energy of **TS32(S)** is 1.03 kcal/mol lower than that of **TS32(R)**, which demonstrates that channel 5 is an energy favorable path. The energy barrier of channel 1 leading to **P1(S)** is 1.58 kcal/mol lower than that of channel 5. Moreover, **P1(S)** is more stable than **P2(S)** in the chloroform solvent. These computed results are in good agreement with the experimental results, which indicates that the reaction processes are nearly not influenced by the solvent.

Conclusions

In this work, six channels for the reaction of 6-benzyl-6-azabicyclo[2.2.1]hept- 2-ene with benzoyl isocyanate have been investigated theoretically using density functional theory. The potential energy surface information has been obtained at the B3LYP/6-31G(d,p) level of theory. We found that, for the title reaction mechanisms, initially, **ZW1** is obtained through the nucleophilic attack by the N1 atom of reactant **A** on the C8 atom of reactant **B** with a barrier of 6.67 kcal/mol. Next, the reaction proceeding along six channels includes two categories: the formally [3,3]-sigmatropic rearrangement and the [4+2] cycloaddition. That is, two channels are formally [3,3]-sigmatropic rearrangements and four channels are [4+2] cycloadditions. Specifically, channels 1 and 4 are two formally [3,3]-sigmatropic rearrangements promoted by the cationic N1 atom of **ZW1**, leading to **P1(S)** and **P2(S)**, respectively. Channels 2, 3, 5, and 6, leading to **P1(S)**, **P1(R)**, **P2(S)**, and **P2(R)**, respectively, are the four [4+2] cycloadditions associated with endo and exo approach modes of the C3−C4 double bond of **Cp** to the two planar conformation of **ZW2**, which are in equilibrium due to the free N1−C8 bond rotation at **ZW2**. The asynchronicity of these P-DA reactions studied in this work are the more favorable two-center interactions between the more nucleophilic center of **Cp**, the C3 or C4 atoms, and the more electrophilic center of **ZW2**, the C2 carbon atom of the cationic iminium framework of **ZW2**.[69] Considering potential energy surfaces and free energy, for **P1**, there are very similar barriers for the formally [3,3]-sigmatropic rearrangement mechanism and the [4+2] cycloaddition mechanism, indicating that the two mechanisms are competitive; for **P2**, the energy favorable pathway is rather the [4+2] cycloaddition processes than the formally [3,3]-sigmatropic rearrangement. Taken together, the main products of this reaction involve **P1** and **P2**, which is in good agreement with the experiment. Moreover, our calculated results demonstrated that solvent effect has no influence on the reaction mechanisms for the title reaction.

Acknowledgment. The work described in this paper was supported by the National Natural Science Foundation of China (No.20672104).

References and Notes

(1) Calderon-Kawasaki, K.; Kularatne, S.; Li, Y. H.; Noll, B. C.; Scheidt, W. R.; Burns, D. H. *J. Org. Chem.* **2007**, *72*, 9081–9087.
(2) Song, Z. L.; Hsung, R. P.; Lu, T.; Lohse, A. G. *J. Org. Chem.* **2007**, *72*, 9722–9731.
(3) Barinka, C.; Byun, Y.; Dusich, C. L.; Banerjee, S. R.; Chen, Y.; Castanares, M.; Kozikowski, A. P.; Mease, R. C.; Pomper, M. G.; Lubkowski, J. *J. Med. Chem.* **2008**, *51*, 7737–7743.
(4) Mereau, R.; Desmedt, A.; Harris, K. D. M. *J. Phys. Chem. B* **2007**, *111*, 3960–3968.
(5) Girardi, G.; Elias, M. M. *Toxicol. Appl. Pharmacol.* **1998**, *152*, 360–365.
(6) Wolman, F. J.; Grasselli, M.; Cascone, O. *Process. Biochem.* **2006**, *41*, 356–361.
(7) Li, H. Q.; Zhu, T. T.; Yan, T.; Luo, Y.; Zhu, H. L. *Eur. J. Med. Chem.* **2009**, *44*, 453–459.
(8) Carpenter, R. D.; Andrei, M.; Aina, O. H.; Lau, E. Y.; Lightstone, F. C.; Liu, R. W.; Lam, K. S.; Kurth, M. J. *J. Med. Chem.* **2009**, *52*, 14–19.
(9) Song, E. Y.; Kaur, N.; Park, M. Y.; Jin, Y.; Lee, K.; Kim, G.; Lee, K. Y.; Yang, J. S.; Shin, J. H.; Nam, K. Y.; No, K. T.; Han, G. *Eur. J. Med. Chem.* **2008**, *43*, 1519–1524.
(10) Ma, Z. D.; Saluta, G.; Kucera, G. L.; Bierbach, U. *Bioorg. Med. Chem. Lett.* **2008**, *18*, 3799–3801.
(11) Cai, Z. W.; Wei, D.; Schroeder, G. M.; Cornelius, L. A. M.; Kim, K.; Chen, X. T.; Schmidt, R. J.; Williams, D. K.; Tokarski, J. S.; An, Y. M.; Sack, J. S.; Manne, V.; Kamath, A.; Zhang, Y. P.; Marathe, P.; Hunt, J. T.; Lombardo, L. J.; Fargnoli, J.; Borzilleri, R. M. *Bioorg. Med. Chem. Lett.* **2008**, *18*, 3224–3229.
(12) Wilkerson, W. W.; Dax, S.; Cheatham, W. W. *J. Med. Chem.* **1997**, *40*, 4079–4088.
(13) Hulten, J.; Andersson, H. O.; Schaal, W.; Danielson, H. U.; Classon, B.; Kvarnstrom, I.; Karlen, A.; Unge, T.; Samuelsson, B.; Hallberg, A. *J. Med. Chem.* **1999**, *42*, 4054–4061.
(14) Frecer, V.; Burello, E.; Miertus, S. *Bioorg. Med. Chem.* **2005**, *13*, 5492–5501.
(15) Ni, B. K.; Zhang, Q. Y.; Headley, A. D. *J. Org. Chem.* **2006**, *71*, 9857–9860.
(16) Yamanaka, M.; Nakagawa, T.; Aoyama, R.; Nakamura, T. *Tetrahedron* **2008**, *64*, 11558–11567.
(17) Fleming, E. M.; Quigley, C.; Rozas, I.; Connon, S. J. *J. Org. Chem.* **2008**, *73*, 948–956.
(18) Peschiulli, A.; Gun'ko, Y.; Connon, S. J. *J. Org. Chem.* **2008**, *73*, 2454–2457.
(19) Zhu, R. X.; Zhang, D. J.; Wu, J.; Liu, C. B. *Tetrahedron-Asymmetry* **2007**, *18*, 1655–1662.
(20) Yang, T.; Ferrali, A.; Sladojevich, F.; Campbell, L.; Dixon, D. J. *J. Am. Chem. Soc.* **2009**, *131*, 9140–9141.
(21) Benyahya, S.; Monnier, F.; Taillefer, M.; Man, M. W. C.; Bied, C.; Ouazzani, F. *Adv. Synth. Catal.* **2008**, *350*, 2205–2208.
(22) Reddy, L. S.; Basavoju, S.; Vangala, V. R.; Nangia, A. *Cryst. Growth. Des.* **2006**, *6*, 161–173.
(23) Blondeau, P.; van der Lee, A.; Barboiu, M. *Inorg. Chem.* **2005**, *44*, 5649–5653.
(24) Lee, R.; Lim, X.; Chen, T.; Tan, G. K.; Tan, C. H.; Huang, K. W. *Tetrahedron Lett.* **2009**, *50*, 1560–1562.
(25) Tsopmo, A.; Ngnokam, D.; Ngamga, D.; Ayafor, J. F.; Sterner, O. *J. Nat. Prod.* **1999**, *62*, 1435–1436.
(26) Cobos, E. S.; Iglesias-Bexiga, M.; Ruiz-Sanz, J.; Mateo, P. L.; Luque, I.; Martinez, J. C. *Biochemistry* **2009**, *48*, 8712–8720.
(27) Leggio, C.; Galantini, L.; Konarev, P. V.; Pavel, N. V. *J. Phys. Chem. B* **2009**, *113*, 12590–12602.
(28) Keuleers, R.; Desseyn, H. O.; Rousseau, B.; Van Alsenoy, C. *J. Phys. Chem. A* **1999**, *103*, 4621–4630.
(29) Aranha, R. M.; Bowser, A. M.; Madalengoitia, J. S. *Org. Lett.* **2009**, *11*, 575–578.
(30) Bowser, A. M.; Madalengoitia, J. S. *Org. Lett.* **2004**, *6*, 3409–3412.
(31) Bowser, A. M.; Madalengoitia, J. S. *Tetrahedron Lett.* **2005**, *46*, 2869–2872.
(32) Wei, D. H.; Tang, M. S. *J. Phys. Chem. A* **2009**, *113*, 11035–11041.
(33) Montero-Campillo, M. M.; Rodriguez-Otero, J.; Cabaleiro-Lago, E. *J. Phys. Chem. A* **2008**, *112*, 2423–2427.
(34) Johnson, L. E.; DuPre, D. B. *J. Phys. Chem. A* **2008**, *112*, 7448–7454.
(35) Moles, P.; Oliva, N.; Safont, V. S. *J. Phys. Chem. A* **2006**, *110*, 7144–7158.
(36) Becke, A. D. *J. Phys. Chem.* **1993**, *98*, 5648–5652.
(37) Chengteh, L.; Weitao, Y.; Parr, R. G. *Phys. Rev. B: Condensed Matter* **1988**, *37*, 785–789.
(38) Florian, J.; Johnson, B. G. *J. Phys. Chem.* **1994**, *98*, 3681–3687.
(39) Zhu, Q.; Lu, Y. X. *Org. Lett.* **2009**, *11*, 1721–1724.
(40) Zhu, Y. Y.; Wang, Y.; Chen, G. J.; Zhan, C. G. *Theor. Chem. Acc.* **2009**, *122*, 167–178.
(41) Lee, E. P. F.; Dyke, J. M.; Chow, W. K.; Chau, F. T.; Mok, D. K. W. *J. Comput. Chem.* **2007**, *28*, 1582–1592.
(42) Tang, Y. Z.; Pan, Y. R.; Sun, J. Y.; Sun, H.; Wang, R. S. *Chem. Phys.* **2008**, *344*, 221–226.
(43) Fukui, K. *Acc. Chem. Res.* **1981**, *14*, 363–368.
(44) Glendening, E. D.; Reed, A. E.; Carpenter, J. E.; Weinhold, F. Included in the GAUSSIAN 03 package of programs, NBO Version 03.01.
(45) Rehbein, J.; Hiersemann, M. *J. Org. Chem.* **2009**, *74*, 4336–4342.
(46) Yoo, H. Y.; Houk, K. N. *J. Am. Chem. Soc.* **1997**, *119*, 2877–2884.
(47) Peles, D. N.; Thoburn, J. D. *J. Org. Chem.* **2008**, *73*, 3135–3144.

(48) Jones, G. O.; Li, X. C.; Hayden, A. E.; Houk, K. N.; Danishefsky, S. J. *Org. Lett.* **2008**, *10*, 4093–4096.
(49) Takano, Y.; Houk, K. N. *J. Chem. Theory Comput.* **2005**, *1*, 70–77.
(50) Frisch, M. J.; Trucks, G. W.; Schlegel, H. B.; Scuseria, G. E.; Robb, M. A.; Cheeseman, J. R.; Montgomery J. A., Jr.; Vreven, T.; Kudin, K. N.; Burant, J. C.; Millam, J. M.; Iyengar, S. S.; Tomasi, J.; Barone, V.; Mennucci, B.; Cossi, M.; Scalmani, G.; Rega, N.; Petersson, G. A.; Nakatsuji, H.; Hada, M.; Ehara, M.; Toyota, K.; Fukuda, R.; Hasegawa, J.; Ishida, M.; Nakajima, T.; Honda, Y.; Kitao, O.; Nakai, H.; Klene, M.; Li, X.; Knox, J. E.; Hratchian, H. P.; Cross, J. B.; Bakken, V.; Adamo, C.; Jaramillo, J.; Gomperts, R.; Stratmann, R. E.; Yazyev, O.; Austin, A. J.; Cammi, R.; Pomelli, C.; Ochterski, J. W.; Ayala, P. Y.; Morokuma, K.; Voth, G. A.; Salvador, P.; Dannenberg, J. J.; Zakrzewski, V. G.; Dapprich, S.; Daniels, A. D.; Strain, M. C.; Farkas, O.; Malick, D. K.; Rabuck, A. D.; Raghavachari, K.; Foresman, J. B.; Ortiz, J. V.; Cui, Q.; Baboul, A. G.; Clifford, S.; Cioslowski, J.; Stefanov, B. B.; Liu, G.; Liashenko, A.; Piskorz, P.; Komaromi, I.; Martin, R. L.; Fox, D. J.; Keith, T.; Al.Laham, M. A.; Peng, C. Y.; Nanayakkara, A.; Challacombe, M.; Gill, P. M. W.; Johnson, B.; Chen, W.; Wong, M. W.; Gonzalez, C.; Pople, J. A. *Gaussian 03*, Revision C.02; Gaussian, Inc.: Wallingford, CT, 2004.
(51) Wang, H. M.; Wang, Y.; Han, K. L.; Peng, X. J. *J. Org. Chem.* **2005**, *70*, 4910–4917.
(52) Domingo, L. R.; Perez-Ruiz, R.; Arguello, J. E.; Miranda, M. A. *J. Phys. Chem. A* **2009**, *113*, 5718–5722.
(53) Arno, M.; Picher, M. T.; Domingo, L. R.; Andres, J. *Chem.—Eur. J.* **2004**, *10*, 4742–4749.
(54) Arno, M.; Zaragoza, R. J.; Domingo, L. R. *Eur. J. Org. Chem.* **2005**, 3973–3979.
(55) Domingo, L. R.; Andres, J.; Alves, C. N. *Eur. J. Org. Chem.* **2002**, 2557–2564.
(56) Parr, R. G.; Szentpaly, V. L.; Liu, S. B. *J. Am. Chem. Soc.* **1999**, *121*, 1922–1924.
(57) Parr, R. G.; Yang, W. Density-Functional Theory of Atoms and Molecules; Oxford University Press: New York, 1989.
(58) Parr, R. G.; Pearson, R. G. *J. Am. Chem. Soc.* **1983**, *105*, 7512–7516.
(59) Domingo, L. R.; Saez, J. A.; Zaragoza, R. J.; Arno, M. *J. Org. Chem.* **2008**, *73*, 8791–8799.
(60) Domingo, L. R.; Aurell, M. J.; Perez, P.; Contreras, R. *Tetrahedron* **2002**, *58*, 4417–4423.
(61) Domingo, L. R.; Chamorro, E.; Perez, P. *J. Phys. Chem. A* **2008**, *112*, 4046–4053.
(62) Domingo, L. R.; Chamorro, E.; Perez, P. *J. Org. Chem.* **2008**, *73*, 4615–4624.
(63) Kohn, W.; Sham, L. J. *Phys. Rev.* **1965**, *140*, 1133–1138.
(64) Perez, P.; Domingo, L. R.; Aurell, A. J.; Contreras, R. *Tetrahedron* **2003**, *59*, 3117–3125.
(65) Domingo, L. R.; Saez, J. A. *Org. Biomol. Chem.* **2009**, *7*, 3576–3583.
(66) Domingo, L. R.; Arno, M.; Saez, J. A. *J. Org. Chem.* **2009**, *74*, 5934–5940.
(67) Jabbari, A.; Houk, K. N. *Org. Lett.* **2006**, *8*, 5975–5978.
(68) Celebi-Olcum, N.; Ess, D. H.; Aviyente, V.; Houk, K. N. *J. Org. Chem.* **2008**, *73*, 7472–7480.
(69) Domingo, L. R. *J. Org. Chem.* **2001**, *66*, 3211–3214.

JP910173D